Computers & Fluids 100 (2014) 176–184

Contents lists available at ScienceDirect

Computers & Fluids

journal homepage: www.elsevier.com/locate/compfluid

Modified SLAU2 scheme with enhanced shock stability

Kalyana Chakravarthy, Debasis Chakraborty *

Directorate of Computational Dynamics, Defence Research and Development Laboratory, Hyderabad 500058, India

ARTICLE INFO

Article history:
Received 12 November 2013
Received in revised form 9 April 2014
Accepted 11 April 2014
Available online 16 May 2014

Keywords:
Shock capturing
Odd–even instability
AUSM schemes

ABSTRACT

Two alternate modifications are proposed to the dissipation term in the mass flux computation of the low dissipation AUSM scheme (SLAU2) developed recently by Kitamura and Shima [1,2]. These modifications are required to remove the odd–even type instability that results in lateral oscillations behind oblique shocks predicted by MUSCL based higher order versions of SLAU2. The first modification involves switching between the original term in SLAU2 and one similar to corresponding term in AUSM^{+}-up. The second modification involves use of density gradient aligned velocity instead of total velocity in SLAU2 (or face normal velocity as in AUSM^{+}-up) in calculation of Mach number that is required for computing this term. It is observed that the second alternative not only delivers better results but also has a more easily differentiable numerical flux that enables easier implicit computations while not altering the simplicity of original SLAU2. The method also renders SLAU2 with a good balance between shock stability and contact capturing ability.

1. Introduction

The Advection Upstream Splitting Method (AUSM) based on cell interface advection Mach number is considered to provide, simultaneously, the accuracy of flux difference splitting methods and the robustness of flux vector splitting methods. It was first proposed by Liou and Steffen [3] and modified several times [4–6] to address the various pathological problems associated with high speed flow solvers. A comprehensive review of AUSM related work was done by Liou [7] and there have also been some more developments since then [6,8]. To minimize numerical dissipation, Shima and Kitamura developed a new AUSM version called SLAU (Simple Low dissipation AUSM) [1,9]. SLAU2 [2] was developed later to deal with the high speed flows and the shock capturing problem. While SLAU2 has many advantages and it is quiet stable, its MUSCL based second order extension predicted saw-tooth type oscillations in density field behind oblique shock for compression ramp. It appears that this susceptibility becomes evident only when numerical shock thickness is low as it is the case in the second order version. It is also possible that the oscillations result from the multidimensional implementation or higher order extension procedure rather than the scheme itself. In a comparative study of many high resolution schemes, Liska and Wendroff [10] showed that while Piecewise Parabolic Method (PPM) [11] is one of the best schemes to capture the fronts in the Woodward–Collela one-dimensional interacting blast waves test problem, it develops unphysical wiggles while a simulating circular blast wave (test case suggested by Toro). Most contact line resolving flux split schemes like HLLC [12] suffer from the so called odd–even instability. EFMO (equilibrium flux method with Osher intermediate states) scheme [13,14] has been shown to be robust even at Mach number of 100 for flow around a cylinder [13], it suffers from odd–even instability [15] in the Quirk test [16]. Shima and Kitamura [17] showed that SLAU with the van Albada limiter predicted post shock oscillations for this same problem which were attributed to pressure difference related damping term becoming zero in supersonic flows. A Shock Detecting SLAU (SD-SLAU) scheme was proposed in which SLAU is replaced by LSHUS (low dissipation simple high resolution upwind scheme) at the shock front as a fix. Although, multidimensional limiting procedures are available [18] to overcome problems associated with increasing spatial order of accuracy, the problem of oscillations in SLAU2 with higher order accuracy is due to the scheme itself rather than the MUSCL procedure. In fact, the same MUSCL procedure was adopted on other schemes to obtain oscillation free solutions.

Several plausible explanations were hypothesized and tested as to why the oscillations appeared when using SLAU2 scheme in the present study. In addition to trying out all known second order TVD limiters, different combination of primitive variables were considered for interpolation in the MUSCL procedure. Reconstruction procedure using interpolation of conserved variables, change in mesh skewness at the corner and a problem with wall boundary conditions which could propagate along the length of the shock

* Corresponding author. Tel.: +91 40 24583310; fax: +91 40 24340037.
E-mail address: debasis_cfd@drdl.drdo.in (D. Chakraborty).

http://dx.doi.org/10.1016/j.compfluid.2014.04.015
0045-7930/

were considered. As a simple solution, a damping term that is a weighted average of the original term in SLAU2 and like one in AUSM$^+$-up was attempted. This approach is more seamless than abrupt switching and was deemed more suited for unsteady simulations with moving shocks. Also, the weights are based on a parameter that characterizes unphysical oscillations rather than a shock sensor. While this procedure was promising in most of the test problems considered, it compromised the normal shock related robustness of the SLAU2 in the Quirk's test [16]. So, an alternative procedure which uses density gradient aligned velocity to calculate Mach number involved in pressure damping term was constructed and tested.

In the following sections, the SLAU2 scheme and the MUSCL scheme are explained. The two proposed modifications to prevent oscillations behind shocks are presented next. The latter modification is shown to suppress unphysical oscillations without losing the established robustness of the SLAU2 scheme. This is demonstrated through simulations of some standard test problems for Euler equations.

2. Numerical method

An explicit second order Runge–Kutta scheme (see Appendix A) was used for temporal integration of the governing equations. For spatial discretization, the SLAU2 scheme from an earlier study [2] was chosen. MUSCL procedure with minmod limiter is used for extension to higher order accuracy in space because it is most dissipative and thus less likely to amplify oscillations. The multidimensional limiting process [18] is a linear multiple of the minmod limiter and, therefore, this limiter is more likely to retain multidimensional monotonicity better than any other.

2.1. SLAU2 scheme

The properties on left and right sides of the face are denoted using subscripts "L" and "R" respectively. The pressure on the face used for computing pressure flux is obtained using the following equations.

$$p_{face} = \frac{p_L + p_R}{2} + \frac{f^+(M_L) - f^-(M_R)}{2}(p_L - p_R) + \frac{\rho_L + \rho_R}{2} c_{1/2}[f^+(M_L) + f^-(M_R) - 1] * \sqrt{\frac{K_L + K_R}{2}} \tag{1}$$

$$f^{\pm}(M) = \frac{(M \pm |M|)}{2M}, \quad if\ |M| \geqslant 1 \qquad = \frac{1}{4}(2 \mp M)(M \pm 1)^2, \quad otherwise \tag{2}$$

In above equations, ρ, p and K denote the density, pressure and specific kinetic energy respectively. M represents face normal Mach number computed using velocity normal to the face and $c_{1/2}$ is interfacial speed of sound. Kitamura and Shima [2] noted that the SLAU2 is not very sensitive to the specification of the interfacial of sound. A simple geometric mean of the values on either sides is used after verifying the fact that replacing it with more complex calculation using critical speed of sound (as in AUSM$^+$-up) has negligible impact on the results. The mass flux across the face is computed using following equations

$$\widehat{M} = \min\left[1, \frac{1}{c_{1/2}}\sqrt{\frac{K_L + K_R}{2}}\right] \tag{3}$$

$$\chi = (1 - \widehat{M})^2 \tag{4}$$

$$g = \max(\min(M_L, 0), -1)\min(\max(M_R, 0), 1) \tag{5}$$

$$|V_n|^+ = (1 - g)|V_n| + g|c_{1/2}M_L| \tag{6}$$

$$|V_n|^- = (1 - g)|V_n| + g|c_{1/2}M_R| \tag{7}$$

$$V_n = c_{1/2}\frac{\rho_L|M_L| + \rho_R|M_R|}{\rho_L + \rho_R} \tag{8}$$

$$\dot{m} = \frac{1}{2}\left[\rho_L(M_L c_{1/2} + |V_n|^+) + \rho_R(M_R c_{1/2} - |V_n|^-)\right] - \frac{\chi}{2}\frac{\Delta p}{c_{1/2}} \tag{9}$$

Δp represents the jump in pressure across the cell face. Velocity vector and total specific enthalpy from upstream side along with mass flux from above equations are used to compute the convective fluxes.

2.2. MUSCL procedure

To extend the order of accuracy, dependent variable values just to the left and right of the face are computed using higher order interpolations. Primitive variables are extrapolated from cell centers to cells faces. Specifically, velocity components, density and temperature are chosen. The results remained almost unchanged when temperature was replaced by pressure. The extrapolation procedure for the face $(i + 1/2, j, k)$ which separates cells (i, j, k) and $(i + 1, j, k)$ on an uniform computational mesh is as follows (indices "j" and "k" are dropped for the sake of clarity).

$$U_L(i + 1/2) = U_i + \frac{\phi(r_L)}{2}[U_{i+1} - U_i] \tag{10}$$

$$U_R(i + 1/2) = U_{i+1} - \frac{\phi(r_R)}{2}[U_{i+1} - U_i] \tag{11}$$

U in above equations represents a primitive variable. r_L and r_R determine the monotonicity of the variables on either sides of the face and are determined using following equations.

$$r_L = \frac{U_i - U_{i-1}}{U_{i+1} - U_i} \tag{12}$$

$$r_R = \frac{U_{i+2} - U_{i+1}}{U_{i+1} - U_i} \tag{13}$$

Higher order computations of face values lead to non-monotonic behavior around sharp fronts, so a limiter function, φ is used to lower the order locally. Negative r indicates non-monotone behavior and the limiter function is set to zero preventing higher order extrapolation. A min-mod limiter which is second-order TVD and also ensures multi-dimensional monotonicity [18] more than any other limiter is used here.

$$\phi(r) = \max(0, \min(1, r)) \tag{14}$$

2.3. Modifications to the damping term in mass flux computation

Stability analyses of shock capturing schemes using simple cases [15,19,20] were reported in several past studies. While most offered insights into the problems, some have offered actual prescriptions. For example, Dumbser and coworkers [21] presented a technique to predict threshold upstream Mach number for triggering odd–even instability for schemes with differential numerical fluxes. Their analysis also pointed to shock upstream region as the origin of the instability thus settling the debate between two contrary views [22,23]. Pandolfi and Ambrosio [19] analyzed many Riemann solvers including some from AUSM family and prescribed how to localize damping to cure carbuncle phenomena. Earlier work by Gressier et al. [15], using linear stability analysis, has shown that strict stability and exact contact line resolution are incompatible for upwind schemes. One can then infer that marginal stability may be preferable if a balance is to be struck. Proving marginal stability itself, however, may not be easy for the non-differentiable fluxes of the AUSM family.

While pursuit of a perfect Riemann solver based on theoretical analyses continues, physical intuition, empirical observations and extensive testing are often the tools adopted to arrive at a robust scheme. Some standards tests like those designed by Quirk [16], Emery [24], etc. help in such regard. Based on such testing, some adhoc fixes are proposed. The fixes [16,19,25,26] mostly involve either combining a baseline accurate scheme with less accurate but a more robust scheme to be used in problematic regions or modifying the dissipation terms. Modification of the internal structure of the numerically predicted shock has also been found to be effective especially in case of AUSM based schemes [20]. This is usually done by appropriate specification of the numerical speed on sound [27,28,6] on the cell faces of finite volume schemes.

SLAU being a recent version of AUSM has not yet been subject to theoretical analysis and difficulties associated with such an exercise are unknown partly because the term in question is not differentiable at sonic point making the whole numerical flux non-differentiable. Schemes with non-differentiable fluxes are not as easily amenable to the kind of analysis done by Dumbser et al. [21]. Numerical experiments were the basis of proposals made here much like in the construction of SLAU and SLAU2 [1,2].

Liou originally argued that pressure jump term in mass flux computation leads to carbuncle phenomena in AUSM and suggested eliminating it completely [29]. However, this term appears in AUSM$^+$−up which was developed later. As noted by Dumbser et al. [21], this conjecture has been refuted in many studies and it is not surprising that this term appears in SLAU and SLAU2 as well. In fact, Shima and Kitamura [9] attempted to remove this term without success and had to retain it. So, no attempt was made remove this term in present work. Instead, modifications were attempted based on their observations and suggestion [30,1,17,9] that dissipation terms along shock normal and parallel direction may need to be considered separately. Forms designed to address oscillations in one-dimensional simulations usually ended up creating problems in multidimensional simulations and vice-versa [9]. These observations along with numerical experimentation provided only path forward since other physical explanations for the odd–even instability have previously been argued to be insufficient [21].

The damping term in mass flux of AUSM$^+$−up uses the average face normal Mach number instead of actual Mach number. So, the damping term can be non-zero even if overall flow is supersonic. Taking a clue from this, Eqs. (3) and (4) were modified as follows in order to suppress the post shock oscillations.

$$\overline{M} = \min\left[1, \sqrt{\frac{M_L^2 + M_R^2}{2}}\right] \tag{15}$$

$$\chi_1 = (1 - \overline{M})^2 \tag{16}$$

2.3.1. SLAU2.1

Post shock oscillations were eliminated by using χ_1 instead of χ in Eq. (9) but that approach creates problem while simulating hypersonic flow around bluff bodies as shown later. So, a weighted average of χ and χ_1 is considered as an option. The present approach of combining two alternate forms of a single term is lot simpler than combining two completely different schemes to get rid of shock instabilities [16,26]. In a way, this approach is similar to one adopted by Ren [25] where extra dissipation is added through the rotated flux mechanism. It is to be noted that the proposed modification adheres to the overall strategy proposed by Shima and Kitamura [17]. In particular, the difference between schemes for computing fluxes for near shocks and elsewhere was to be kept minimal. Here, in fact there is only one scheme. Only one term is modified as per local requirements.

The weighted average approach rather than abrupt switching is more seamless and stable as verified through some unsteady flow simulations. The weight should be biased toward χ_1 when unphysical oscillations are present. An unphysical oscillation is easily detected using the values of r_L and r_R computed in the MUSCL procedure. If both are negative, there are two neighboring extrema which constitutes unphysical behavior. So, the weight is defined as:

$$\omega = \frac{1}{1 + \exp[2.5 \max(r_L, r_R)]} \tag{17}$$

$$\chi' = \omega\chi_1 + (1 - \omega)\chi \tag{18}$$

χ' in above equation is used to replace χ in Eq. (9). For high positive values of r_L and r_R, ω is negligible, χ' is close to χ and the method is closer to original SLAU2. Near two neighboring extrema, χ' is closer to χ_1. This gradual switching technique proved to more stable than abrupt switching. The weighting function proposed here is much simpler than a shock sensor based switching function. Quirk [16] demonstrated the effectiveness of switching techniques using standard test problems but left out a detailed discussion of shock sensors. For complex problems, however, the accuracy or robustness may be limited by how shock is detected. Earlier work was based on Harten switch and Jameson sensor [31] but more recent work on shock detection (done for combining dissipative and non-dissipative schemes for performing direct numerical simulations or large eddy simulations of high speed flows) is based on mostly Ducros sensor [32] and its variant [33] or more recent alternatives [34,35]. Shock detection does not seem to have been perfected yet – a fact evident from the tunable parameters in almost all the sensors. Though this switching/merging function is simpler, there is a numerical parameter in Eq. (17) whose value was determined using a series of test problems. Its use goes against the original SLAU2 design philosophy. But a single value seems to produce acceptable results for all the test problems. At least, problem specific adjustment does not seem to be necessary. Genin [36] combined HLLE [37] and HLLC [12] schemes using switching technique to capture contact lines while avoiding shock instabilities. HLLE was used on faces aligned with shock normals while HLLC was the baseline scheme. This technique was demonstrated using a Quirk type test involving normal shocks. It is to be noted that shock normal and parallel directions are obvious in that test (performed using very slightly perturbed but almost cartesian mesh with the shock). When the same technique was applied to hypersonic flow simulation around a cylinder involving a bow shock, the results are not as good as those reported by Quirk [16] using a similar switching technique of resorting to HLLE normal to the shock. The better results of Quirk are not surprising since the locations where HLLE is used could be determined a priori based on knowledge of the nature of desired solution. The adjustable parameter in the shock sensor was also chosen through experimentation. Quirk outlined a procedure for determining the tunable parameter suggesting that it may depend on pre-shock Mach number. It, clearly, is not easily applicable to unsteady flows. Genin's predictions may be improved by using gradual rather than abrupt switching but that would require characterization of graduation. Distance from the shock in normal direction seems to be a sensible parameter for this but it may be hard to compute in course of unsteady simulations.

2.3.2. SLAU2.2

While the previous modification was able to eliminate oscillations behind oblique shocks and worked well for most test cases, it reduced the robustness of SLAU2 in capturing a normal shock in the Quirk test [16]). The probable reason is that the proposed change does not effectively pre-empt the formation of two neighboring extrema. A more effective and, if possible, simpler pressure jump term that automatically adjusts to the local requirements (based on shock direction) was sought. Use of Mach number computed using velocity normal to the shock in the damping term is an obvious choice because the post shock normal Mach number is always below unity and damping term will be non-zero. That way, damping term is directionally dependent just as needed and the robust normal shock capturing ability of SLAU2 could perhaps be extended to oblique/curved shocks.

Shock normal direction can be detected in several ways. This information is also needed in construction rotated Riemann solvers which determine total flux as a combination of a shock-aligned and tangential fluxes that are computed differently [38,25,26]. Levy and coworkers [38] investigated three different angles for upwind differencing. Their first choice is the flow direction, which in the present instance amounts to using the actual Mach number (based on total velocity), results in the original SLAU2 scheme. The other two choices are pressure gradient and velocity magnitude gradient directions which were shown to be equivalent for detecting shock waves. They prescribed velocity magnitude gradient direction because their study was intended to improve accuracy rather than robustness of shock capturing. This choice was expected to help in that regard in presence of shear waves. Nishikawa and Kitamura [26] use the velocity difference (computed from left and right) vector which also aligns with shock normal and is parallel to shear but is not really equivalent to using velocity magnitude gradient vector as claimed by the authors. One of the key goals of the present work was to keep SLAU2 intact to the extent possible and that included keeping unchanged the resolution of shear waves by SLAU2. Either pressure gradient or density gradient can be used to detect shock normal direction. The use of latter can be useful in detecting contact lines in addition to shocks. In anticipation of problems that may arise in resolving contact lines, density gradient direction was chosen. Results were found to change insignificantly in most problems if pressure gradient direction was chosen instead. Eqs. (3) and (4), respectively, are replaced by the following equations.

$$\widetilde{M} = \min\left[1, \sqrt{\frac{M_{L,\rho}^2 + M_{R,\rho}^2}{2}}\right] \tag{19}$$

$$\chi'' = (1 - \widetilde{M})^2 \tag{20}$$

$M_{L,\rho}$, $M_{R,\rho}$ represent the Mach numbers on either sides calculated using velocities aligned with their respective density gradients and interfacial speed of sound.

For one-dimensional cases, these equations are equivalent to Eqs. (3) and (4) respectively. So the results for one-dimensional Riemann test problems [10] including the 1.5 shock test [1], would be no different from those obtained using the original SLAU2. Just as in case of rotated Riemann solvers [25,26], the modification is intended to deal with multidimensional instabilities.

In the low Mach number limit, the density gradients are negligible but have non-zero values. The total Mach number and density aligned Mach number are different. However, both χ and χ'' are almost equal and the modified scheme would be very close to the original SLAU2. For problems involving inclined shocks, the Mach number based on shock normal velocity is always below unity behind the shock which implies that χ'' is non-zero thus providing damping to kill transverse oscillations. With minimal changes to the SLAU2 scheme, there is automatic adjustment to both shock normal and parallel requirements. This modification is demonstrated to be better than the previous one in the next section. This modification unlike the previous alternative does not involve a numerical parameter and is, therefore, preferable even if the two modifications work equally well.

3. Results

In this section, simulations that illustrate the baseline scheme's problem with oblique shock predictions including those performed to rule out any artifacts are presented first. The modifications for fixing the problem are then tested. Hypersonic flow around circular cylinder and Double Mach reflection problems are considered for illustrating the effectiveness of the proposed modifications. These two of these are standard test cases for carbuncle phenomenon. While this phenomenon results mostly in unphysical behavior ahead of the shock, there can also be post shock oscillations along either directions. Double Mach reflection is a good test case for checking the so called kinked Mach stem problem that plagues many Riemann solvers. In addition, it also has a triple point which may create problem for combined schemes or the weighted averaging approach in the present work. The Emery test case also has a triple point, an expansion fan intersecting a shock and two slip lines. This is a good test case for checking contact line capturing ability. The modifications did not seem to change the results in any significant way worth noting for other test problems considered.

Several other problems were also considered for testing the proposed modifications but are not discussed here. The list included the Rankine vortex problem [17,9], circular blast wave, Quirk test problem, Emery test problem and other two-dimensional Riemann problems [10].

The results obtained with SLAU2.1 were almost identical to those of original SLAU2. The differences arise only when unphysical oscillations are detected. Otherwise, the first proposed modification is of no consequence. SLAU2.2, on the other hand, may actually produce different results from SLAU2 for problems where the pressure difference related damping terms in the two are different. No differences are expected at contact lines. If the contact line is normal to the flow (like in shock tube type problems), the velocity is fully aligned with the density gradient everywhere and both schemes have the same damping terms. Besides there is no pressure jump across a contact line and so the pressure difference term is also minimal. For this reason, there will no difference even when the contact lines is along the flow direction (i.e., the last term in Eq. (9) is negligible because Δp is small). By this logic, it can be concluded that the differences will arise in flows which have zones where (i) there are pressure gradients and (ii) density gradients are not aligned with the flow direction. One such problem involving a non-aligned shear wave was used previously as a test case for the rotated Riemann solver [26]. The mixing between the two streams involves both density and pressure gradients that are not aligned to the flow directions. Unequal velocities lead to shear as well. The rotated Riemann solver of Nishikawa and Kitamura [26] uses direction sensor that is sensitive to shear unlike in SLAU2 where flow alignment with density gradient is more relevant. This problem actually can be used to study both effects of shear as well as density gradient. Another problem with such conditions is a stationary compressible vortex where pressure gradient balances the centrifugal force. The flow is along tangential direction while pressure and density gradients are along the radial direction. Solutions for these two problems are computed with proposed modifications and compared to baseline SLAU2 and the rotated HLL solver [26].

3.1. Flow around corners

A test case involving both convex and concave corners was chosen instead of a simple flow over a ramp. This is a slight variation of the test problem chosen by Levy et al. [38] for testing their rotated Riemann solvers. A straight channel was bent at an angle of $\tan^{-1}(0.2)$ to create these corners at a fixed axial location. The inflow Mach number was set to 3.0. The expansion fan and shock generated at these corners respectively intersect away from the wall. Some solvers that capture oblique shocks accurately might predict oscillations if the shock happens to intersect an expansion fan [39]. Fig. 1 shows the density isolevels predicted by second order version of SLAU2 using a 240×100 mesh. The grid is cartesian upstream of the corner and is skewed downstream. Post shock oscillations along the direction of the shock are clearly evident. χ is zero everywhere in the flow in this simulation. Since a finite volume scheme was used here, the pressure boundary conditions are prescribed at face centers.

Since boundary curvature is zero at all cell faces of the mesh, zero gradient boundary conditions is used for pressure. There is usually no problem with this approach. Still, to ensure that the oscillations are not a result of a problem that originates at the corner and propagates along the length of the shock, χ is the replaced by χ_1 while computing transverse fluxes on the first 20 faces close to the lower wall. Results from this exercise are shown in Fig. 2. This change supresses the oscillations near the wall but further away, where the original SLAU2 scheme is retained, oscillations are generated. So, the instability problem seems inherent to the SLAU2 scheme. To also prove that the oscillations do not result from sudden change in the mesh metrics at the corner, the problem is simulated in a different way. Supersonic inflow at a non-zero angle was prescribed as boundary condition to a constant area channel. At one corner of the inflow boundary, a shock is generated while an expansion fan is generated at the other. In this case also, but with a perfectly cartesian mesh, the post shock oscillations were generated as shown in Fig. 3. It is not clear that these oscillations are related to odd–even instability. The odd–even instability is considered a failing of the baseline scheme and not a result of the procedure for attaining higher order accuracy. Here, of course, baseline first order code does not have this problem. It is to be noted in this context that thicker numerically predicted shocks are generally less susceptible to multidimensional instabilities (flux difference splitting schemes which produce much crisper shocks are much more susceptible to shock instabilities compared to flux vector splitting schemes that produce thicker shocks). So, it is not surprising that the oscillations appear only when higher order extension is attempted in order to thin down the numerical shock thickness.

Fig. 4(a) and (b) show the density isolevels predicted using the two modifications proposed here. The post shock oscillations are effectively supressed by using either of the two. If χ_1 is used to calculate the damping term instead of the weighted average, no oscillations appear behind the shock. But that results in unphysical oscillations in case of hypersonic flow around a circular cylinder.

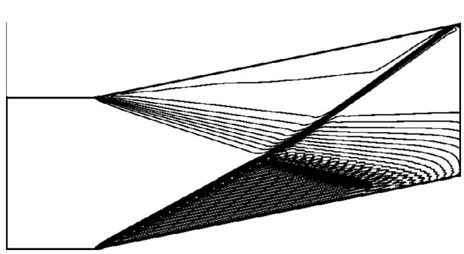

Fig. 1. Density isolevels predicted by SLAU2 scheme for Mach 3.0 flow through a bent channel.

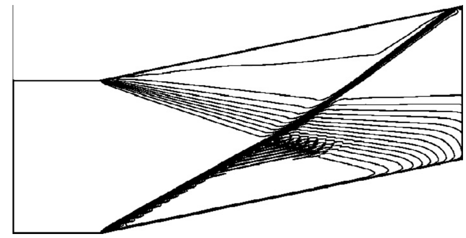

Fig. 2. Density isolevels predicted by SLAU2 scheme for Mach 3.0 flow through a bent channel with post shock oscillations suppressed close to the wall.

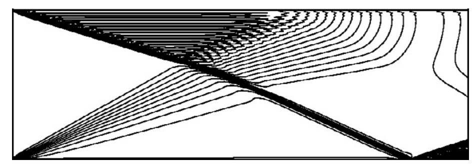

Fig. 3. Density isolevels predicted by SLAU2 scheme for Mach 3.0 flow through a channel with inflow entering at an angle.

The other drawback is that the damping term based on face normal Mach number may change abruptly depending on the mesh orientation. The contour levels of χ_1 are shown in Fig. 5. When the mesh orientation changes at the corner, there is an abrupt change in damping term when there are no gradients in the flow. Such abrupt changes in mesh metrics are detrimental toward accuracy but are sometimes unavoidable in flow geometries of engineering interest. This sudden change in damping might lead to some numerical artifacts when the flow, unlike in present case, is non-uniform.

3.2. Hypersonic flow around a cylinder

Fig. 6(a) shows the density isolevels for Mach 10 flow around a circular cylinder predicted by SLAU2 using a 80×120 mesh and χ_1 to compute the pressure jump related damping term. Unphysical oscillations around the stagnation streamline are clearly evident. Instead of replacing χ altogether, if the weighted expression based on unphysical oscillation detector proposed in Eq. (18) is used, proper solution as in Fig. 6(b) on par with one obtained using original SLAU2 is obtained. When density gradient aligned Mach number is used instead of the weighted average, there is very slight improvement in the solution which is plotted in Fig. 6(c). Also, the temperature contours (not shown here) were better predicted when compared to the combined HLLC/E scheme with a shock sensor developed by Genin [36]. Density profiles along the radial line and the surface predicted using SLAU2.2 are compared to corresponding solutions of SLAU2 in Figs. 7 and 8 respectively. The predictions of SLAU2.1 are completely indistinguishable from those of SLAU2 and are, therefore, left out. The predictions in both plots differ by less 0.4%. SLAU2 and SLAU2.2 underpredict the stagnation density by about 0.7% and 0.9% respectively when compared to a theoretical estimate. The errors are of the same order as 1% error reported for SLAU [9] at Mach 8 for this problem.

One concern about compound schemes (including rotated solvers) is the convergence to steady state. The residuals tend to level off with iterations and do not fall as rapidly as in case of individual schemes [38,26]. So, the direction vectors used to combine the two schemes are frozen after the residual falls below a chosen value to accelerate further decrease. Nishikawa and Kitamura [26] argue that this is of not of much concern in unsteady flows. However, residuals leveling off at rather high values indicate the presence of oscillations in time. To rule out such a possibility, the residuals

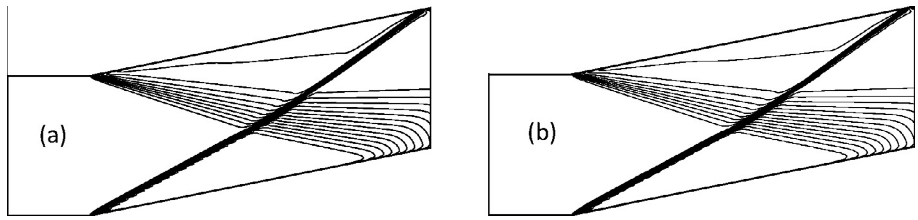

Fig. 4. Density isolevels for Mach 3.0 flow through a bent channel (a) SLAU2.1 scheme and (b) SLAU2.2 scheme.

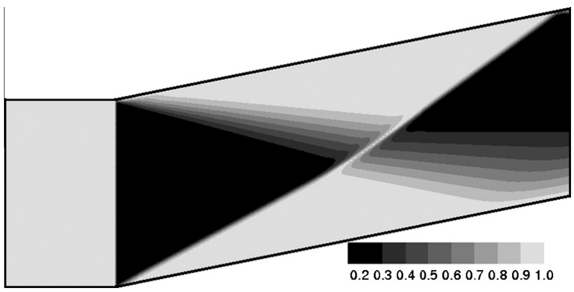

Fig. 5. Distribution of χ_1 in the pressure jump damping term on transverse faces for Mach 3.0 flow through a bent channel.

are plotted for all three version of the SLAU2 scheme in Fig. 9. Residuals level off at much lower values with the suggested modifications. Robustness is achieved here by introducing additional damping as needed just as in case of rotated Riemann solvers. So, better convergence is to be expected. It is somewhat unclear why this is not the case with rotated Riemann solvers.

3.3. Double Mach reflection

This test is intended to check if solvers create a kinked Mach stem, an unphysical artifact that appears due to insufficient transverse dissipation [15]. A Mach 5.5 shock wave moves up a ramp of 30° creating a double Mach stem with a shock triple point. At the foot of the shock on the inclined surface, some solvers [15,16] create an unphysical triple point supposedly resulting from a jet of fluid hitting it from the upstream side [9]. The density isolevels predicted by the original SLAU2 scheme and the second modified version proposed here are shown in Fig. 10(a) and (b) respectively. No kinked Mach stem or a hint of it is seen in both the results. A 180 x 100 mesh, roughly the same as 200×100 mesh used by Gressier et al. [15] in their comparative study, was used for the simulations. Unlike the results using EFM in that study, there is a hint of a jet hitting the shock on the inclined wall. So, SLAU2 is accurate enough for shear waves to capture this feature.

The original SLAU2 predicts some post shock tranverse oscillations that the modified version does not. Such oscillations were also reported earlier by Shima and Kitamura [9] although their simulations were done with a Mach number of 10 and with much greater resolution, both of which, would make a shock more susceptible to instabilities, if any. In fact, the double Mach reflection case was simulated with a shock moving at Mach number of 1.7 to compare with high resolution WAF-HLLC results reported in literature. No unphysical oscillations were observed in the original SLAU2 predictions for this case.

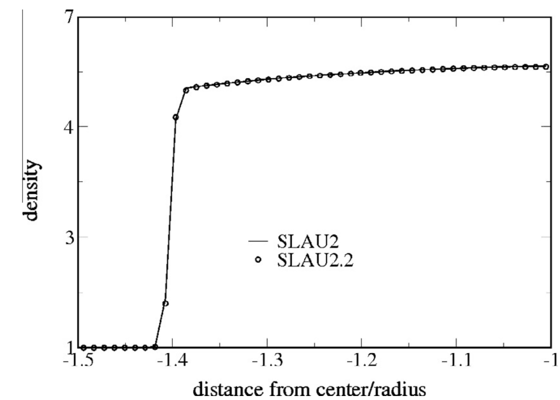

Fig. 7. Density variation along the stagnation stream for Mach 10 flow around a cylinder.

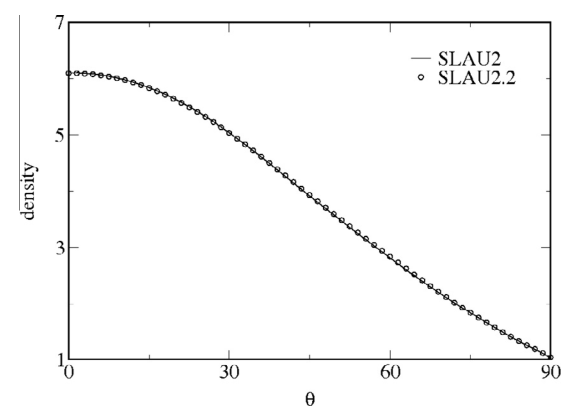

Fig. 8. Density variation on the surface as function of angle for Mach 10 flow over a circular cylinder. 0° corresponds to the stagnation point.

3.4. Shear wave problem

This problem involves steady flow from left to right through a square domain of unit size. The inflow conditions for top and bottom halves are specified as follows.

$$(\rho, u, v, p)_{top} = (0.25, 4.0, 0, 0.25) \tag{21}$$

$$(\rho, u, v, p)_{bottom} = (1.0, 2.4, 0, 0.5) \tag{22}$$

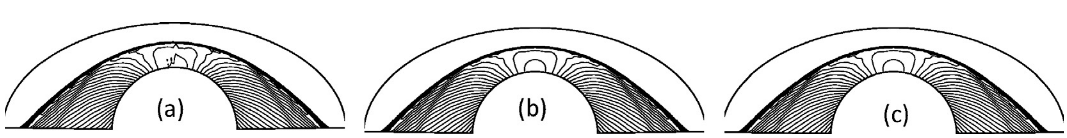

Fig. 6. Density isolevels for hypersonic flow in front of a circular cylinder (a) SLAU2 using χ_1 to compute pressure jump related damping term, (b) SLAU2.1 and (c) SLAU2.2.

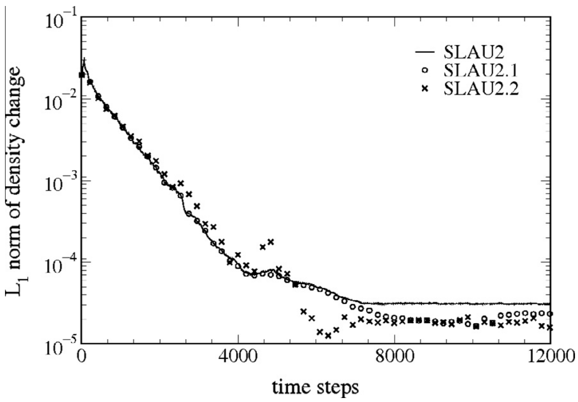

Fig. 9. Convergence of various schemes.

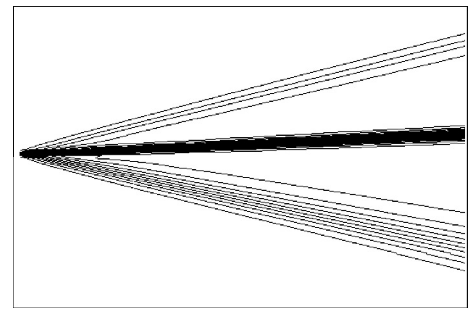

Fig. 11. Density isolevels for shear wave problem.

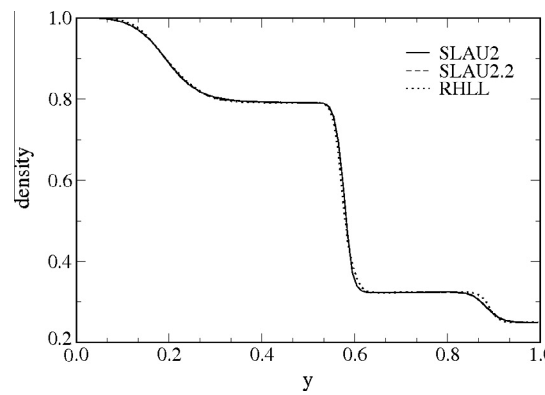

Fig. 12. Density profiles at the exit for the shear wave problem.

Zero gradient conditions are used at upper and lower boundaries while simple extrapolation is used at the right boundary. The mixing between the two streams involves both density and pressure gradients that are not aligned to the flow directions. Unequal velocities lead to shear as well. The rotated Riemann solver of Nishikawa and Kitamura [26] uses direction sensor that is sensitive to shear unlike in SLAU2 where flow alignment with density gradient is more relevant. This problem actually can be used to study both effects of shear as well as density gradient. The solutions are computed using baseline SLAU2 and the two proposed modified versions along with the RHLL solver [26] on a 100 $\times$ 100 mesh. Nishikawa and Kitamura [26] used double the resolution and first order schemes for computing the reported solutions. The present study is based completely on second order schemes and direct comparison with their predictions is not possible. Solution computed using a second order version of RHLL is used here instead. The solution contains a contact line in the middle of the domain that is slightly misaligned with the abscissa and two inclined shocks originating at the same point on the left boundary. Density isolevel plot made from solution of SLUA2.2 scheme is shown in Fig. 11. This plot is indistinguishable from one made using SLAU2. The shocks facilitate equilibration of pressure around the contact line with imposed pressures of top and bottom boundaries. The density variations along the vertical line at the exit are plotted in Fig. 12. SLAU2.1 results are once again left out since they coincide with those of SLAU2. The results of SLAU2 and SLAU2.2 appear to be very similar at this scale. Density and pressure gradients exist only near shocks just as in previous problems. At least, this test case helps establish that the SLAU2.2 does not generate any unphysical behavior at the triple point. Both SLAU2 and SLAU2.2 capture contact line as well as the rotated solver although the latter captures shocks are crisply. Numerical shock thickness is known to be slightly higher in case of SLAU2 when compared to flux difference splitting schemes and other AUSM versions and the same is true with its modified versions as well.

3.5. Effect of modifications on numerical dissipation

Low dissipation is a key desirable feature of SLAU schemes. Specifically, it does not suffer from the D'Alemdert paradox (non-zero drag prediction for circular cylinder in low speed inviscid flow). As argued previously, in the limit of zero Mach number, the modifications proposed here are inconsequential. The numerical dissipation of both SLAU2.1 and SLAU2.2 would be same as in original SLAU2 and much lower than other shock capturing schemes. This is demonstrated by simulating the Taylor Green vortex problem. Low dissipation of SLAU2 has already been established using other problems but this problem is particularly relevant if SLAU2 is to be considered for large eddy simulations where numerical viscosity should be kept minimal. Later, a highly compressible test case is presented, where SLAU2.2 has different dissipation characteristics is discussed.

3.5.1. Low Mach number test case: Taylor Green Vortex

The numerical viscosities associated with different scheme have been estimated using the Taylor Green vortex problem by fitting the functional forms of viscous solutions to inviscid numerical

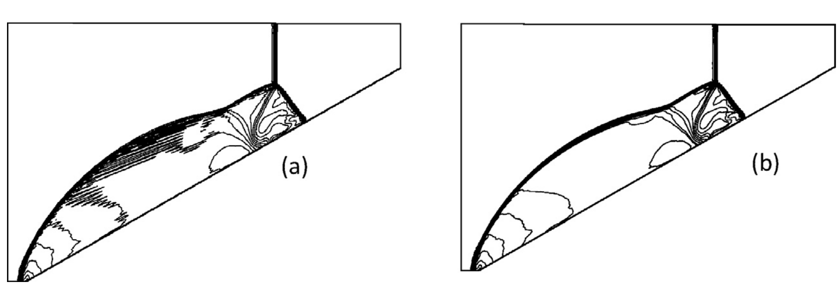

Fig. 10. Density isolevels for Mach 5.5 shock traveling up a 30° ramp (a) SLAU2 and (b) SLAU2.2.

solutions. The computed numerical viscosities (ν) for three different grid resolutions (N) are compared with those of RHLL scheme [26] in Fig. 13. It is clear from the figure that numerical dissipation of SLAU2.2 is order of magnitudes lower than those of RHLL. The results of SLAU2.1 and original SLAU2 are indistinguishable from those from SLAU2.2.

3.5.2. High Mach number test case: Stationary compressible isentropic vortex

This test case which has a steady state analytical solution [40] is often used to verify the high resolution capability of weighted essentially oscillatory (WENO) or other schemes intended for turbulence computations. This case is more relevant for present study than the Rankine vortex problem that was used earlier to establish low dissipation nature of SLAU2. That is because, the damping term in SLAU2 and SLAU2.2 become identical in the limit of zero Mach number. Differences would appear only at high subsonic Mach numbers. The following equations constitute a steady state solution for this problem.

$$u = \varepsilon\tau e^{\alpha(1-\tau^2)} \sin\theta \tag{23}$$

$$v = -\varepsilon\tau e^{\alpha(1-\tau^2)} \cos\theta \tag{24}$$

$$T = -\frac{(\gamma-1)\varepsilon^2 e^{2\alpha(1-\tau^2)}}{4\alpha\gamma} \tag{25}$$

where τ is the distance from the center of the vortex non-dimensionalized by the critical radius of the vortex (=0.05). The parameters $\alpha = 0.204$ and $\varepsilon = 0.8$ quantify the radial spread and intensity of the vortex. Density and pressure are computed using isentropic flow relations. The flow is in tangential direction while density and pressure gradient are along radial direction. So χ'' would be unity everywhere. The intensity of the vortex is increased (compared to previous studies on high resolution scheme and shock-vortex interactions where ε has a much lower value) to make the flow highly compressible and bring out the differences between predictions of SLAU2.2 and the original SLAU2. The peak Mach number is roughly around 0.8. χ, which is used to compute pressure difference related damping term approaches zero. The differences in solutions result mainly from differences in values of χ'' (used in SLAU2.2) and χ (used in SLAU2). To have quantitative comparison of numerical dissipation of various schemes, the radial profiles of density on a uniform 100×100 mesh at time of 10 is presented in Fig. 14. At this time, there is significant decay of the vortex due to numerics. The decay rate associated with RHLL is much higher than any of the SLAU2 versions. Unlike in case of Rankine vortex simulations reported earlier [9], where a Roe scheme destroyed

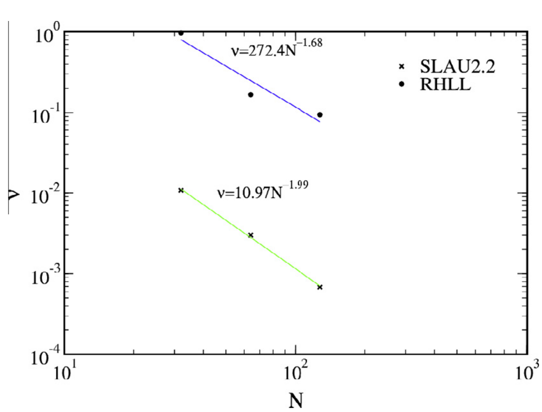

Fig. 13. Comparison of numerical viscosities of RHLL and SLAU2.2.

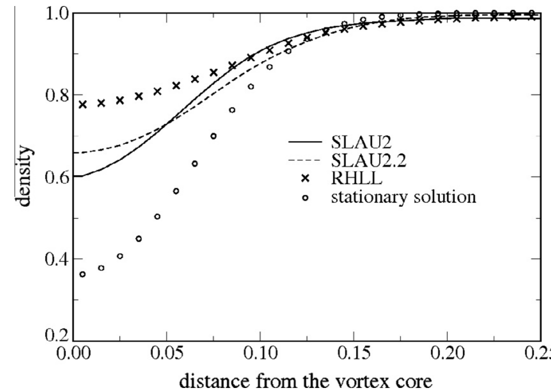

Fig. 14. Radial density profiles for the compressible vortex problem with various schemes.

the axisymmetric nature of the solution, all schemes here including RHLL retain it. At first glance, SLAU2.2 seems to predict faster decay than SLAU2 but that is only in the core region dominated by rigid body type rotation. Beyond the core (critical radius), the decay seems actually lower in SLAU2.2 predictions. This, however, does not necessarily imply less numerical dissipation of SLAU2.2 in this region. Once the vortex starts to decay, initial balance between the pressure gradient and centrifugal force is lost and velocity fields develop a small radial component. The initial difference between SLAU2.2 and SLAU2 is due to the damping term but the subsequent divergence may depend on the inherent dynamics of the flow. Also, the decay in case of both SLAU2 versions is likely due to the limitations of the MUSCL approach. Combining SLAU2 schemes with a higher order interpolation schemes for computing face values may actually lower dissipation to levels acceptable for turbulence computations.

4. Conclusions

Two modifications were proposed to the SLAU2 scheme in order to eliminate transverse post shock oscillations under certain conditions. The first was arrived at using an idea borrowed from the AUSM$^+$-up scheme while the second was motivated by a suggestion from original developers of SLAU2 scheme that different damping treatments are needed along shock normal and parallel directions. This has been achieved by an automatic adjustment of a single term rather than using two different schemes like in case of SD-SLAU [17] or rotated Riemann solvers [38,26]. The more robust latter modification depends on density gradient as a measure of how a face aligns with a shock rather than adjustable parameter dependent complex shock sensors in combined schemes of the past. No unphysical behavior was predicted while using this approach at intersection points of multiple shocks. There is no hint of carbuncle phenomena, kinked Mach stems or other pathological problems associated with Riemann solvers. SLAU2.2 proposed here is mostly designed to fix the problem of oscillations behind oblique shocks. In some canonical test problems (like double Mach reflection test case), however, there is no sign of instability behind normal shocks.

The low numerical dissipation of SLAU2 scheme makes it good choice for large eddy simulations of supersonic flows. The numeric caused decay in the compressible vortex problem could possibly be reduced by replacing MUSCL approach with a higher order interpolation scheme like PPM, an adaptive limiter [41] or a WENO scheme. For this, hybridization with a non-dissipative higher order scheme or adaptive limiters [41] are needed. Work in this direction is being pursued and will be reported in the future. The contact resolving ability of the scheme is also expected to be useful for modelling mixing and flames in combustors.

Appendix A

The second order Runge Kutta method used for time integration is this work for a set of differential equations $dy/dt = f(y)$ is summarized as follows.

$$y^* = y^n + dt\, f(y^n)$$

$$y^{n+1} = (y^n + y^*)/2 + dt\, f(y^*)/2$$

where "n" and "$n+1$" denote current and next time steps and "dt" is the time step.

References

[1] Shima E, Kitamura K. On new simple low-dissipation scheme of AUSM-family for all speeds, AIAA paper 2009-136.
[2] Kitamura K, Shima E. Improvements of simple low-dissipation AUSM against shock instabilities in consideration of interfacial speed of sound. In: ECCOMAS CFD, Lisbon, Portugal; 2010.
[3] Liou MS, Steffen C. A new flux splitting scheme. J Comput Phys 1993;107:23–39.
[4] Liou MS. A sequel to AUSM: AUSM+. J Comput Phys 1996;129:364–82.
[5] Kim KH, Kim C, Rho O. Methods for the accurate computations of hypersonic flows i. AUSMPW+ scheme. J Comput Phys 2001;174:38–80.
[6] Liou MS. A sequel to AUSM, Part II: AUSM+-up. J Comput Phys 2006;214:137–70.
[7] Liou MS. Ten years in the making – AUSM family, AIAA paper 2001-2521.
[8] Chang C, Liou MS. A robust and accurate approach to computing compressible multiphase flow: stratified flow model and AUSM+up scheme. J Comput Phys 2007;225:840–73.
[9] Shima E, Kitamura K. Parameter-free simple low-dissipation AUSM family scheme for all speeds. AIAA J 2011;49(8):1693–709.
[10] Liska R, Wendroff B. Comparison of several difference schemes on 1d and 2d test problems for the Euler equations. SIAM J Sci Comput 2003;25:995–1017.
[11] Colella P, Woodward PR. The piecewise parabolic method (ppm) for gas-dynamical simulations. J Comput Phys 1984;54:174–201.
[12] Toro EF, Spruce M, Speares W. Restoration of the contact surface in the HLL-Riemann solver. Shock Waves 1994;4:25–34.
[13] Moschetta J-M, Pullin DI. A robust low diffusive kinetic scheme for the Navier–Stokes/Euler equations. J Comput Phys 1997;133:193–204.
[14] Pullin DI. Direct simulation methods for compressible inviscid ideal gas flow. J Comput Phys 1980;34:231–44.
[15] Gressier J, Moschetta J-M. Robustness versus accuracy in shock wave computations. Int J Numer Method Fluids 2000;33:313–32.
[16] Quirk JJ. A contribution to the great Riemann solver debate, ICASE, Report No 92-64.
[17] Shima E, Kitamura K. On AUSM-family scheme for all speeds with shock detection for carbuncle-fix, AIAA paper 2009-3544.
[18] Gerlinger P. Multi-dimensional limiting for high-order schemes including turbulence and combustion. J Comput Phys 2012;231:2199–228.
[19] Pandolfi M, D'Ambrosio D. Numerical instabilities in upwind methods: analysis and cures for the "carbuncle" phenomenon. J Comput Phys 2001;166:271–301.
[20] Chauvat Y, Moschetta JM, Gressier J. Shock wave numerical structure and the carbuncle phenomenon. Int J Numer Method Fluids 2005;47:903–9.
[21] Dumbser M, Moschetta JM, Gressier J. A matrix stability analysis of the carbuncle phenomenon. J Comput Phys 2004;197:647–70.
[22] Wada Y, Liou M-S. An accurate and robust flux splitting scheme for shock and contact discontinuities. SIAM J Sci Comput 1997;18:633–57.
[23] Xu K, Li Z. Dissipative mechanism in Godunov-type schemes. Int J Numer Method Fluids 2001;37:1–22.
[24] Emery AE. An evaluation of several differencing methods for inviscid fluid flow problems. J Comput Phys 1968;2:306–31.
[25] Ren Y. A robust shock capturing scheme based on rotated Riemann solvers. Comput Fluids 2003;32:1379–403.
[26] Nishikawa H, Kitamura K. Very simple, carbuncle-free, boundary layer resolving, rotated hybrid Riemann solvers. J Comput Phys 2008;227:2560–81.
[27] Edwards JR, Liou MS. Low-diffusion flux-splitting methods for flows at all speeds. AIAA J 1998;36:1610–7.
[28] Liou MS, Edwards JR. Numerical speed of sound and its application to schemes for all speeds, AIAA paper 99-3268.
[29] Liou MS. Probing numerical fluxes: mass flux, positivity and entropy satisfying property, AIAA paper 97-2035.
[30] Kitamura K, Roe P, Ismail F. Evaluation of Euler fluxes for hypersonic flow computations. AIAA J 2009;47(1):44–53.
[31] Jameson A, Schmidt W, Turkel E. Numerical simulation of Euler equations by finite volume methods using Runge–Kutta time stepping schemes, AIAA paper 81-1250.
[32] Ducros F, Ferrand V, Nicoud F, Weber C, Darracq D, Gacherieu C, et al. Large Eddy simulation of the shock turbulence interaction. J Comput Phys 1999;152:517–49.
[33] Bhagatwala A, Lele SK. A modified artificial viscosity approach for compressible turbulence simulations. J Comput Phys 2009;228:4965–9.
[34] Hill DJ, Pullin DI. Hybrid tuned center difference WENO method for large eddy simulations in the presence of strong shocks. J Comput Phys 2004;194:435–50.
[35] Visbal MR, Gaitonde DV. Shock capturing using compact differencing based methods, AIAA paper 2005-1265.
[36] Genin F. Study of compressible turbulent flows in supersonic environment by large eddy simulation, Ph.D. thesis, Georgia Institute of Technology, Atlanta, GA, USA; 2009.
[37] Einfeldt B, Munz CD, Roe PL, Sjoreen B. On Godunov-type methods near low densities. J Comput Phys 1991;92:273–95.
[38] Levy DW, Powell KG, van Leer B. Use of a rotated Riemann solver for the two-dimensional Euler equations. J Comput Phys 1993;106:201–14.
[39] Zhang S, Shu C-W. Convergence towards steady state solutions of the Euler equations with WENO schemes, Tech. Rep. 2006–6, Scientific Computing Group, Brown University, Providence, RI, USA; 2006.
[40] Shu C. High order finite difference and finite volume WENO schemes and discontinuous Galerk in methods for CFD, Tech. Rep. 2001–11, ICASE (NASA); 2001.
[41] Billet G, Louedin O. Adaptive limiters for improving the accuracy of the MUSCL approach for unsteady flows. J Comput Phys 2001;170:161–83.